Optical reflectivity and electron mass enhancement in expanded liquid caesium

1997 J. Phys.: Condens. Matter 9 2693

(http://iopscience.iop.org/0953-8984/9/13/006)

J. Phys.: Condens. Matter **9** (1997) 2693–2698. Printed in the UK PII: S0953-8984(97)77201-1

Optical reflectivity and electron mass enhancement in expanded liquid caesium

B Knuth†, F Hensel† and W W Warren Jr‡

† Institute of Physical Chemistry, Marburg University, Marburg, Germany
‡ Department of Physics, Oregon State University, Corvallis, OR, USA

Received 16 August 1996

Abstract. Optical reflectivity data are reported for expanded liquid caesium over the range 144 °C (density, 1778 g cm^{-3}) to 1100 °C (density, 1.195 g cm^{-3}) for photon energies 0.5 eV$\leqslant \hbar\omega \leqslant$ 3.8 eV. Optical effective mass ratios obtained from the plasma frequency are compared with mass ratios extracted from analysis of the magnetic susceptibility. Both masses exhibit enhancements for liquid densities less than about 1.3 g cm^{-3}, suggesting that expanded caesium gradually transforms to a highly correlated metal below this density.

1. Introduction

One of the most general characteristics of simple metals is the small change observed in most electronic properties when the metal is melted. For the alkali metals as well as many polyvalent metals such as aluminium, lead, copper, and indium, basic properties such as the electrical conductivity or magnetic susceptibility change by only a few per cent on passing from the crystalline solid to the liquid state [1]. This well known characteristic of simple metals is usually explained, first, by the fact that the short-range atomic correlations and atomic volume in the liquid near the melting temperature (T_m) are closely similar to those of the crystal. Second, for most metals the ionic charges are so well screened by the high density of conduction electrons that the absence of long-range order in the ionic potentials of the liquid is relatively unimportant and *both* liquid and solid can be reasonably well described by a model of nearly free electrons. The strong screening of Coulomb potentials also applies to electron–electron interactions, whose effects are relatively small in ordinary high-density metals.

In contrast to solids, however, the volume of liquid metals can be expanded by large factors when the liquids are heated toward the liquid–gas critical point. The critical density of the alkali metals, for example, is only about 20% of the density of the liquid at T_m. The 'expansion' of liquid metals on heating is, however, not a true expansion of the interatomic distance in a fixed structure, as occurs in solids. Rather, as shown by recent neutron [2] and x-ray scattering experiments [3], the dominant effect is a decrease of the average *number* of near neighbours with a relatively weak increase of the distance between neighbours. The large reduction of density near the critical point leads to dramatic changes in electronic properties such as the electrical conductivity [4], magnetic susceptibility [5, 6], and various nuclear magnetic resonance (NMR) features [7]. The magnetic properties, in particular, reveal the increasing importance of electron–electron interactions (correlation) as the density and conduction electron screening are reduced.

0953-8984/97/132693+06$19.50

In this paper we describe an exploration of the effects of large density reduction on the optical properties of liquid caesium. We report experimental results for the optical reflectivity of liquid caesium from near the melting point at atmospheric pressure ($T_m = 30\,^\circ$C, $\rho_m = 1.84$ g cm^{-3}) to a temperature/pressure point ($T = 1100\,^\circ$C, $P = 45$ bar) where the density $\rho = 1.19$ g cm^{-3}. For reference the critical parameters of caesium are $T_c = 1651\,^\circ$C, $P_c = 92.5$ bar, and $\rho_c = 0.38$ g cm^{-3}. We analyse the reflectivity data to extract an electron effective mass which shows the onset of a low-density enhancement in remarkably good agreement with enhanced masses extracted from the magnetic susceptibility data [7, 8].

2. Experimental methods and results

For high-temperature optical studies of liquid caesium, it is necessary to confine the sample material in a cell with an appropriate optical window. The window must offer the widest possible spectral transparency range together with high resistance to corrosion by the hot metal. The best available window material for high-temperature studies of caesium is single-crystal sapphire, which offers a spectral range of roughly 0.5 eV$< \hbar\omega <$ 3.8 eV. The high-temperature limit of our experiments was determined by the onset of sapphire corrosion above about 1200 °C.

In order to have a clean sample–sapphire interface special care was taken to remove adsorbed oxygen from the sapphire windows. For this purpose the sapphire was heated inside a glovebox up to 1200 °C for several hours and the cell was assembled in the glovebox directly after this cleaning procedure. However, it must be pointed out that the purity of the caesium metal was not better than 99.93% so that trace amounts of oxygen contamination of the metal cannot be excluded.

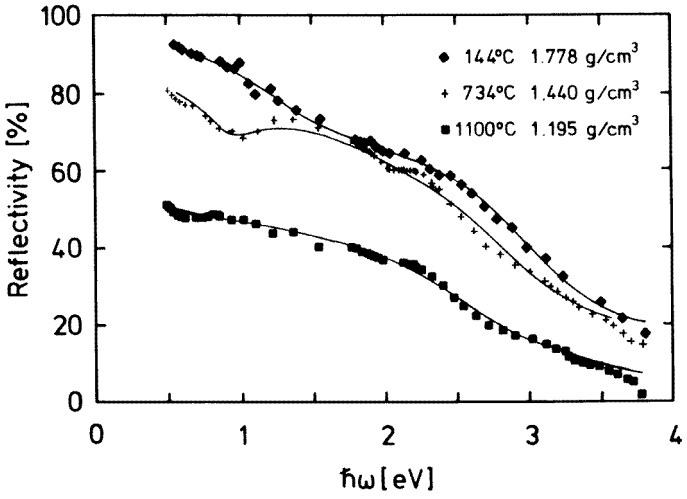

Figure 1. Reflectivity spectra $R(\omega)$ versus $\hbar\omega$ for expanded liquid caesium at three temperature–pressure points. The solid lines represent the fit to the model function (1).

The reflectivity was measured for ten temperatures covering a density range of 1.2–1.8 g cm^{-3}. Typical reflectivity spectra $R(\omega)$ versus $\hbar\omega$ for three selected temperatures

and densities are presented in figure 1. These data exhibit the typical characteristics of materials with metallic electron concentrations. The most obvious of these is the relatively high reflectivity in the infra-red and visible range and a decrease to low reflectivity values in the near ultra-violet.

Two additional features are evident in the reflectivity spectra. At the lower temperatures, a broad 'shoulder' reveals absorption at about 1.5 eV. This feature is well known from studies of solid caesium [9, 10] and has been identified as an interband transition between electronic states of s- and p-like atomic symmetry. The persistence of this feature in the liquid state offers another example of the close relationship between the electronic structure of the crystal and that of the liquid near T_m. The interband feature gradually becomes indistinguishable at higher temperatures, but here a new feature develops at slightly lower energy, about 1.0 eV. This lower-energy feature has been seen in other alkali metals [11, 12] both solid and liquid. Its origin is most probably due to caesium suboxides [13], which may be enriched at the interface [14].

To analyse the reflectivity data further, we have used a simple model [15] to extract the optical constants $\epsilon(\omega)$ and $\epsilon_2(\omega)$. Introduction of a model is necessary because the limited energy range of the data prohibits use of the usual Kramers–Kronig analysis to obtain the real and imaginary parts of the dielectric constant $\epsilon(\omega)$. The following model function was chosen:

$$\epsilon(\omega) = \epsilon_\infty - \frac{\omega_{p0}^2}{\omega(\omega + i\Gamma_0)} - \sum_{l=1} \frac{\omega_{pl}^2}{\omega(\omega + i\Gamma_l) - \omega_l^2}. \tag{1}$$

In (1), ω_{pl}, ω_l, and Γ_l are the plasma frequency, angular frequency, and width of the lth oscillator, respectively, and the contribution of high-energy excitations to the dielectric function is ϵ_∞. The second term in (1) represents the contributions of nearly free electrons within the Drude model parameterized by ω_{p0} and Γ_0. Fits of the model function (1) to the experimental reflectivity curves are shown in figure 1. The extracted behaviour of the real and imaginary dielectric constants $\epsilon_1(\omega)$ and $\epsilon_2(\omega)$ is shown in figure 2.

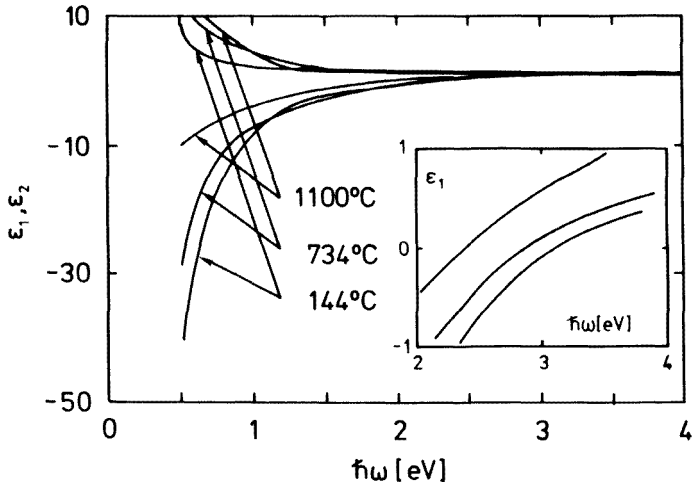

Figure 2. Real (lower curves) and imaginary (upper curves) dielectric constants, $\epsilon_1(\omega)$ and $\epsilon_2(\omega)$ respectively, extracted using the model function (1) as described in the text. Inset, behaviour of $\epsilon_1(\omega)$ near $\epsilon_1 = 0$ used to extract the plasma frequency ω_p.

In terms of our interest in the evolution of the electronic structure at low density, the most important of the parameters is the plasma frequency

$$\omega_p^2 = 4\pi n_e e^2 / m_{eff} \tag{2}$$

which, given the value of the electron density n_e, provides a measure of the effective mass m_{eff}. Since $\epsilon_2(\omega)$ is very small near the plasma resonance, ω_p is determined quite accurately by the condition $\epsilon_1(\omega_p) = 0$ (inset, figure 2). Values of m_{eff} expressed as the mass ratio $m^* = m_{eff}/m_0$ are plotted in figure 3 and compared with mass ratios extracted from the magnetic susceptibility [6–8].

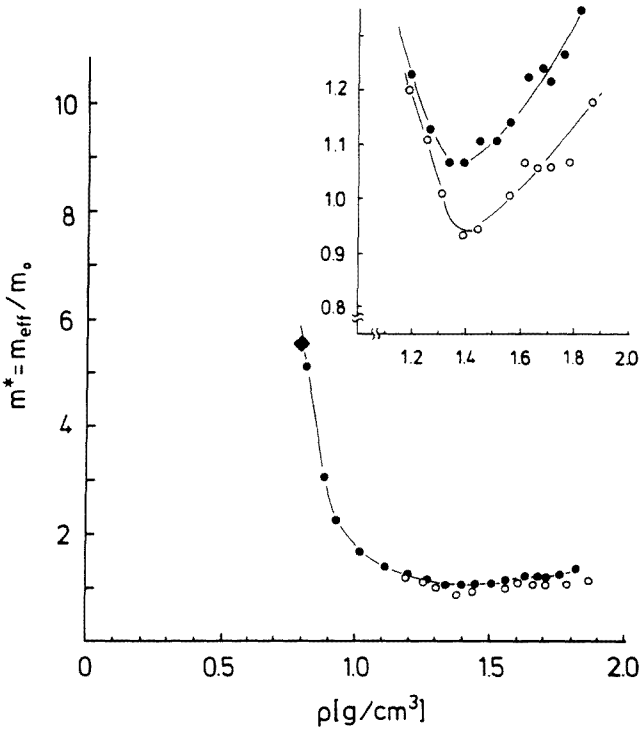

Figure 3. Density dependence of mass ratio $m^* = m_{eff}/m_0$ extracted from optical reflectivity (open circles) and magnetic susceptibility (solid circles). The solid diamond at lowest density is the value calculated in [8]. The solid line is a guide to the eye. Inset, a detailed comparison of optical and magnetic mass ratios in the region of the enhancement onset.

Like the 'magnetic' masses, the optical masses at high liquid densities are reasonably close to the free electron value, i.e. $m^*_{opt} \approx 1.15$. However, as the density falls below about 1.3 g cm^{-3} ($n_e \approx 6 \times 10^{21}$ cm^{-3}), the optical mass ratio begins to increase. This onset of optical mass enhancement coincides with changes in the density dependence of a number of magnetic parameters [7] and, in particular, agrees with the variation of the magnetic mass. This point, at which the density is about two-thirds of that of the solid or the liquid at the melting point, represents the onset of significant modification of the electronic properties by electron correlation effects.

3. Discussion

In the absence of a detailed theory of interacting electrons in an expanded liquid metal, approximate models must be invoked to obtain even a qualitative understanding of the mass enhancement effects. One line of description is derived from the perspective of solid state physics. Brinkman and Rice [16] as well as Mott [17] have argued that in a highly correlated metal near the metal–nonmetal transition there should develop a mass enhancement $m^* \approx \frac{1}{2}f$ where f is the instantaneous fraction of doubly occupied atomic sites. This model is usually applied to a half-filled band metal such as a (fictitiously) expanded alkali metal crystal or solid atomic hydrogen.

Application of concepts derived for a crystal to a *liquid* metal can be justified, at least in a qualitative sense, by the fact that many properties of liquid metals near their melting points are closely similar to the corresponding properties of the metals below T_m. For example, the volume of caesium increases by only 2.5% on melting and the electrical conductivity decreases by 40% [1]. Of particular relevance to the present work, we note that the total magnetic susceptibility of caesium changes by 9% at T_m [18] while the optical mass ratios are 1.29 in the solid [19] and 1.19 in the liquid state near T_m [9]. Such results emphasize the fact that the basic electronic structure is most strongly influenced by factors such as the atomic volume and the average number of near neighbours which are similar above and below T_m, while they are relatively insensitive to the absence of long-range order in the liquid. This includes, in particular, the effect of the d states on the density of electronic states at the Fermi level, $N(E_F)$. Band structure calculations [20] suggest that the initial decrease of m^* with density above T_m is due to a reduction of the contribution from the d states.

At still lower densities, however, NMR Knight shift and spin–lattice relaxation measurements [7] show clearly that the character of the susceptibility changes and that the spin susceptibility becomes enhanced by correlations. The present results show that this correlation enhancement is revealed as well by the behaviour of the optical response and that the optical mass begins to increase in the same density range as the magnetic mass.

An alternative approach is to view the expanded liquid as the high-density limit of a compressed metal vapour. Redmer and Warren [21] recently analysed the magnetic susceptibility of fluid caesium from this point of view. This treatment describes the fluid as a mixture of discrete chemical species such as atoms (Cs^0), monomeric ions (Cs^+), and neutral dimers ($(Cs_2)^0$), as well as thermally ionized free electrons. Despite the oversimplification of the model, in particular the neglect of atomic correlation ('liquid structure'), this model yields a reasonable representation of the temperature- and density-dependent spin susceptibility. The susceptibility enhancement in this model arises from the presence of paramagnetic species such as Cs^0 and $(Cs_2)^+$. Localization of electrons in such species, of course, corresponds to an increase in the effective mass or, equivalently, a reduction in the electronic mobility.

The relationship of these two very different approaches may be seen as follows. The Brinkman–Rice highly correlated metal corresponds to the chemical equilibrium

$$2Cs^0 \rightarrow Cs^+ + Cs^- \tag{3}$$

being shifted far to the left. Now, as Mott has argued [17], the mass enhancement is equivalent to a reduction in the number of current carriers due to the localization of singly occupied sites, i.e. formation of Cs^0. The effect on the electrical conductivity is to replace m by m^* in the expression $\sigma = ne^2\tau/m$ while retaining the number of carriers equal to the number of atoms, i.e. $n = n_{\text{atoms}}$. The conductivity is proportional to the concentration of

doubly occupied sites [Cs^-]. Comparing this concentration to its value in the uncorrelated limit, [Cs^-] = [Cs^+] = 0.5, we have

$$1/m^* = [Cs^-]/0.5 \tag{4}$$

which is the Brinkman–Rice result $m^* = \frac{1}{2}f$ with $f = [Cs^-]^{-1}$. Thus the Brinkman–Rice model corresponds to a chemical equilibrium model in which thermal ionization and cluster formation are not included.

Acknowledgments

Support of this work by the Deutsche Forschungsgemeinschaft and the Fonds der Chemischen Industrie is gratefully acknowledged. WWW is partially supported by the Alexander von Humboldt Stiftung.

References

[1] See, for example, Shimojii M 1977 *Liquid Metals* (London: Academic)
[2] Winter R, Bodensteiner T, Gläser W and Hensel F 1987 *Ber. Bunsenges. Phys. Chem.* **91** 1327
[3] Tamura K and Hosokawa S 1993 *J. Non-Cryst. Solids* **156–8** 646
[4] Pilgrim W-C, Winter R and Hensel F 1993 *J. Phys.: Condens. Matter* **5** 183
[5] Freyland W 1979 *Phys. Rev.* B **20** 5104
[6] Warren W W Jr 1984 *Phys. Rev.* B **29** 7012
[7] Warren W W Jr, Brennert G F and El-Hanany U 1989 *Phys. Rev.* B **39** 4038
[8] Chapman R G and March N H 1988 *Phys. Rev.* B **38** 792
[9] Smith N V 1970 *Phys. Rev.* B **2** 2840
[10] Fäldt A and Neve J 1983 *Solid State Commun.* **45** 399
[11] Mayer J and Hietel B 1966 *Proc. Int. Coll. on Optical Properties and the Electronic Structure of Metals and Alloys* (Amsterdam: North-Holland) p 47
[12] Overhauser A W and Butler M A 1976 *Phys. Rev.* B **14** 3371
[13] Metsch G, Bauhofer W and Simon A 1985 *Z. Naturf.* a **40** 303
[14] Adamson A W 1976 *Physical Chemistry of Surfaces* (New York: Wiley)
[15] Verleur H W 1968 *J. Opt. Soc. Am.* **58** 1356
[16] Brinkman W F and Rice T M 1970 *Phys. Rev.* B **2** 4302
[17] Mott N F 1974 *Metal–Insulator Transitions* (London: Taylor and Francis) ch 4
[18] Collings E W 1965 *Phys. Kondens. Mater.* **3** 335
[19] Ham F S 1962 *Phys. Rev.* **128** 82
[20] Warren W W Jr and Mattheiss L F 1984 *Phys. Rev.* B **30** 3103
[21] Redmer R and Warren W W Jr 1993 *Phys. Rev.* B **48** 14 892